52. Formisano V et al. *Science* **306** 1758 (2004)
53. Ehlmann B L et al. *Science* **322** 1828 (2008)
54. Ehlmann B L, Mustard J F, Murchie S L *Geophys. Res. Lett.* **37** L06201 (2010)
55. McCleese D J et al. *J. Geophys. Res. Planets* **112** E05S06 (2007)
56. McCleese D J et al. *J. Geophys. Res. Planets* **115** E12016 (2010)
57. Heavens N G et al. *J. Geophys. Res. Planets* **116** E04003 (2011)
58. Poulet F et al. *Nature* **438** 623 (2005)
59. Murchie S et al. *J. Geophys. Res. Planets* **112** E05S03 (2007)
60. Korablev O I, Bertaux J-L *Solar Syst. Res.* **37** 441 (2003) [*Astron. Vestn.* **37** 483 (2003)]
61. Bertaux J-L *J. Geophys. Res. Planets* **111** E09S01 (2006)
62. Chang I C *Appl. Phys. Lett.* **25** 370 (1974)
63. Korablev O et al. *Adv. Space Res.* **29** 143 (2002)
64. Korablev O et al. *J. Geophys. Res. Planets* **111** E09S03 (2006)
65. Formisano V et al. *Planet. Space Sci.* **53** 963 (2005)
66. Bertaux J-L et al. *Nature* **435** 790 (2005)
67. Bertaux J-L et al. *Science* **307** 566 (2005)
68. Bertaux J L et al. *J. Geophys. Res. Planets* **117** E00J04 (2012)
69. Fedorova A A et al. *Icarus* **219** 596 (2012)
70. Fedorova A et al. *J. Geophys. Res. Planets* **111** E09S07 (2006)
71. Perrier S et al. *J. Geophys. Res. Planets* **111** E09S06 (2006)
72. Lebonnois S et al. *J. Geophys. Res. Planets* **111** E09S05 (2006)
73. Lefèvre F et al. *Nature* **454** 971 (2008)
74. Head J W et al. *Nature* **434** 346 (2005)
75. Levrard B et al. *Nature* **431** 1072 (2004)
76. Fedorova A et al. *J. Geophys. Res. Planets* **111** E09S08 (2006)
77. Trokhimovskiy A et al., in *39th COSPAR Scientific Assembly, 14–22 July 2012, Mysore, India*, Abstract D2.1-19-12, p. 2005
78. Fedorova A A et al. *Icarus* **200** 96 (2009)
79. Maltagliati L et al. *Science* **333** 1868 (2011)
80. Maltagliati L et al. *Icarus* **223** 942 (2013)
81. Maltagliati L et al. *Icarus* **213** 480 (2011)
82. Fouchet T et al. *Icarus* **190** 32 (2007)
83. Tschimmel M et al. *Icarus* **195** 557 (2008)
84. Korablev O et al., in *Second Workshop on Mars Atmosphere Modelling and Observations, February 27–March 3, 2006, Granada, Spain* (Eds F Forget et al.) (Paris, 2006) p. 244
85. Korablev O, in *37th COSPAR Scientific Assembly, 13–20 July 2008, Montréal, Canada*, p. 1580
86. Fedorova A A et al. *Icarus* **208** 156 (2010)
87. Smith M D *Annu. Rev. Earth Planet. Sci.* **36** 191 (2008)
88. Zasova L V et al. *Cosmic Res.* **44** 305 (2006) [*Kosm. Issled.* **44** 319 (2006)]
89. Wolkenberg P et al. *Icarus* **215** 628 (2011)
90. Krasnopolsky V A, Maillard J P, Owen T C *Icarus* **172** 537 (2004)
91. Mumma M J et al. *Bull. Am. Astron. Soc.* **36** 1127 (2004)
92. Mumma M J et al. *Science* **323** 1041 (2009)
93. Geminale A, Formisano V, Giuranna M *Planet. Space Sci.* **56** 1194 (2008)
94. Geminale A, Formisano V, Sindoni G *Planet. Space Sci.* **59** 137 (2011)
95. Krasnopolsky V A *Icarus* **217** 144 (2012)
96. Villanueva G L et al. *Icarus* **223** 11 (2013)
97. Zahnle K, Freedman R S, Catling D C *Icarus* **212** 493 (2011)
98. Lefèvre F, Forget F *Nature* **460** 720 (2009)
99. Webster C R et al. *LPI Contrib.* (1719) 1366 (2013)
100. Zurek R W et al. *Planet. Space Sci.* **59** 284 (2011)
101. Abrams M C et al. *Appl. Opt.* **35** 2774 (1996)
102. von Clarmann T et al. *J. Geophys. Res. Atmos.* **108** 4736 (2003)
103. Bernath P F et al. *Geophys. Res. Lett.* **32** L15S01 (2005)
104. Kasuya M, Nakajima M, Hamazaki T *Trans. Space Technol. Jpn.* **7** (ists26) To_4_5 (2009)
105. Korablev O I, Bertaux J-L, Vinogradov I I *Proc. SPIE* **4818** 272 (2002)
106. Korablev O I et al., in *Proc. of the 5th Intern. Conf. on Space Optics, ICSO 2004, 30 March–2 April 2004, Toulouse, France* (ESA SP-554, Ed. B Warmbein) (Noordwijk: ESA Publ. Division, 2004) p. 73
107. Nevejans D et al. *Appl. Opt.* **45** 5191 (2006)
108. Korablev O I et al. *J. Opt. Technol.* **78** 317 (2011) [*Opt. Zh.* **78** (5) 44 (2011)]
109. Korablev O et al. *Appl. Opt.* **52** 1054 (2013)
110. Korablev O I et al. *Solar Syst. Res.* **46** 31 (2012) [*Astron. Vestn.* **46** 34 (2012)]
111. Drummond R et al. *Planet. Space Sci.* **59** 292 (2011)
112. Korablev O et al., in *39th COSPAR Scientific Assembly, 14–22 July 2012, Mysore, India*, Abstract E2.6-22-12, p. 969
113. Korablev O I *Phys. Usp.* **48** 626 (2005) [*Usp. Fiz. Nauk* **175** 655 (2005)]

PACS numbers: **07.57.–c**, **84.40.–x**, **89.20.–a**
DOI: 10.3367/UFNe.0183.201307i.0769

A new-generation interferometer for fundamental and applied research

A V Ipatov

1. Introduction

A design of a four-element very long baseline interferometer (VLBI) has been developed at the Institute of Applied Astronomy, Russian Academy of Sciences, for use in fundamental and applied research. Observations with this device are expected to provide millimeter-accurate data on Earth orientation parameters (EOPs) and station locations, as well as to determine the universal time used in the Global Navigation Satellite System (GNSS).

The fundamental scientific tasks regarding radio interferometers are to provide positioning and timing support and navigation services or, more specifically,

— to establish and maintain a celestial reference frame in the form of the catalogued positions of extragalactic radio sources;

— to establish and maintain a terrestrial reference frame in the form of the catalogued positions and velocities of reference stations;

— to determine orientation parameters between the terrestrial and celestial reference frames (Earth rotation parameters);

— to establish dynamic frames as ephemerides of Solar System bodies;

— to refine the national coordinated time UTC (SU) scale and keep it within prescribed limits with respect to the universal coordinated time (UTC) scale;

— to develop signal propagation models for the atmosphere and ionosphere.

We note that the current precision and efficiency requirements for the positioning and timing and navigation support in applied problems are often comparable to those for the fundamental positioning and timing support. For example, the error in extracting navigation data from GNSS signals should not exceed 30 cm (for the fundamental segment, this value decreases to 3 cm!). This level of accuracy implies that the ERP determination and prediction system should provide an accuracy of 0.1 ms for the pole coordinates and nutation and precession angles and an

A V Ipatov Institute of Applied Astronomy, Russian Academy of Sciences, St. Petersburg, Russian Federation
E-mail: ipatov@ipa.nw.ru

Uspekhi Fizicheskikh Nauk 183 (7) 769–777 (2013)
DOI: 10.3367/UFNr.0183.201307i.0769
Translated by E G Strel'chenko; edited by A M Semikhatov

Table 1. Indicators and factors of the Federal Program "Support, Development and Operation of the GLONASS for 2012–2020."

Item	Indicators and factors	2011	2015	2020
2.6	Earth rotation parameter error			
2.6.1	Pole coordinates in a real-time regime, m	0.06	0.06	0.006
2.6.2	Pole coordinates in an a posteriori regime, m	0.03	0.03	0.002
2.6.3	Universal time in a real-time regime using Russian-made equipment, ms	0.07	0.07	0.02
2.6.4	Universal time in an a posteriori regime, ms	0.03	0.03	0.01
2.6.5	Precession and nutation parameters, m	0.01	0.01	0.003
2.8	SGRF* error			
2.8.1	SGRF and ITRF** transformations parameters, m	0.5	0.06	0.01
2.8.2	GLONASS-implemented SGRF, m	0.2	0.1	0.02
2.8.3	Relative link of FAGN*** points, m	0.05	0.01	0.005

* SGFF — State Geocentric Reference Frame.
** ITRF — International Terrestrial Reference Frame.
*** FAGN — Fundamental Astronomic Geodetic Network.

accuracy of 10 μs for the universal time [1]. We note that the observational session should be repeated at least 3–4 times a day. Target indicators of the Federal Program "Support, Development and Operation of the GLONASS System for 2012–2020" [2] (see Table 1) serve best to illustrate these points.

In Russia, problems like these are currently being handled by the Russian very long baseline interferometry (VLBI) network "Quasar" operating within the International VLBI Service for Geodesy and Astronomy, IVS. The "Quasar" facilities contributing to IVS include three observatories, a correlator, processing and analysis centers, and the VLBI instrumentation development center.

Based on "Quasar" observations, the pole coordinates and the precession and nutation angles are measured weekly with an error less than 0.001 arc s. Universal time with an error less than 70 μs is determined daily at six-hour intervals in a nearly real-time regime [3].

Operating within the international VLBI service, "Quasar" serves to provide Russia with data on the International Terrestrial Reference Frame (ITRF), the International Celestial Reference Frame (ICRF), and the Earth rotation parameters. The accuracies involved are as follows:

— celestial reference frame: 100 μas for ICRF sources;

— terrestrial reference frame: 5 mm for ITRF stations;

— Earth rotation parameters [4]: 100 μas for the pole coordinates and nutation and precession angles, and 10 μs for the universal time;

— troposphere parameters: 5 mm.

The "Quasar" radio astronomy observatories in the village of Svetloe, Leningrad region; village of Zelenchukskaya, Republic of Karachaevo-Cherkessia; and Badary, Republic of Buryatia are among 15 basic reference stations in the Global Geodesic Observing System (GGOS) project. A basic reference station is defined as one that hosts next-generation space geodetic instruments (including VLBI and Satellite Laser Ranging (SLR) together with Global Navigation Satellite System (GNSS) receivers and, if possible, a DORIS antenna (DORIS standing for Doppler Orbitography and Radio-positioning Integrated by Satellite), the reference points of space station observation instruments being connected by parameters that have the same or better accuracy as the reference frame.

There are recommendations from the international GGOS community on how to support and develop hardware and software tools for the reference stations of the global geodetic infrastructure [5]. Reference stations with their own infrastructure are supposed to provide quantitative information for determining and monitoring the reference source coordinates in the celestial and terrestrial frames, as well as information on Earth's rotation parameters, sea level, water circulation, climate, and natural disaster hazards.

The international VLBI service, in turn, has designed a radio interferometry development project, VLBI-2010 [6], under which the accuracy of the fundamental frames and Earth's rotation parameters is envisaged to be improved dramatically to a level of a few millimeters (Table 2). The project imposes some requirements on potentially promising IVS stations. The desired technical characteristics of the next-generation telescopes are shown in Table 3.

As can be seen, the GLONASS target indicators are close to the fundamental theoretical requirements and entirely consistent with the interferometry trends developed by the international VLBI service. Listed below are the principles that should be followed in the development of a new Russian domestic interferometer:

— the new radio interferometer should have its telescopes fully compatible with the "Quasar" telescopes;

— the project should rely on the VLBI-2010 working group results;

— radio environment at the telescope sites is an important factor to account for;

— telescope surveillance should be 24 hours a day 7 days a week;

— the longitude spacing of telescopes should be maximized.

The operating frequency range of the radio interferometer is chosen so as to correspond to the "Quasar" operating frequencies and with a view for the prospected transition to a higher-frequency range to extend the frequency range of registered signals and to enable collaboration with the telescopes in Germany and Spain within international programs.

Table 2. VLBI project results and their expected precision.

Results	Parameter	Value
Pole coordinates (x_p, y_p)	Precision Reception rate Time resolution Observation schedule	25 μas 24 hrs 10 min – 1 hr 24 hr every day
Universal time (UT1 – UTC)	Precision Reception rate Time resolution Observation schedule	2 μs 24 hrs 10 min 24 hr every day
Nutation angles	Precision Reception rate Time resolution Observation schedule	25 μas 24 hrs 24 hrs once a week
Celestial reference frame	Precision Observation schedule	0.15 mas 1 month
Terrestrial reference frame	Precision	2 mm

There will be three stages in the implementation of the project. At the first stage, we will register about a 300 MHz wide single band in the 2.2 GHz range (S band) in order to measure the ionospheric delay and three closely spaced 512 MHz bands in the 8.0–9.5 GHz range (X band) in order to measure the group delay. With two-bit quantization, four registration channels and two polarizations, the data flow from each radio telescope will be 16 Gbps. The group delay will be determined up to about 4 ps.

Our plan for the second stage is to register a single 500 MHz wide band in the 7–9 GHz range (X band) for determining the ionospheric delay and three 500 MHz bands in the 28–34 GHz (Ka band) with a synthesized band of 6 GHz for determining the group delay. The group delay determination accuracy will be about 2 ps. The new radio interferometer will have two telescopes located at the Badary and Zelenchukskaya observatories of the "Quasar" network. The third and fourth radio telescopes are to be located in the regions of Ussuriisk and Kaliningrad in order for the universal time to be determined more accurately for the GLONASS.

The component facilities of the next-generation radio-interferometer include: an antenna system, receivers, a broad-band eight-channel digital signal acquisition system, a data buffering and transfer system, a frequency timing system, a software correlator for data processing, and a system for measuring the electrical characteristics of the atmosphere.

2. Radio interferometer antenna system

An IVS-recommended 13.2 m antenna system (AS) from Vertex Antennentechnik GmbH (Germany) (see Fig. 1) has been adopted for the radio interferometer under construction, with the parameters listed in Table 4.

3. Radio telescope reception system

Radio telescope receivers are located in a focal cabin. The triband feed [7] and the input amplifiers are placed in a cryostat and cooled to liquid hydrogen temperature using a closed-cycle cryogenic microcooler. The electromagnetic waves focused by the antenna pass through a radio-transparent coating into the cryostat, where they are collected by the feed, separated by frequency ranges (S, X, and Ka) and polarizations, summed with the phase and amplitude calibration signals from the calibration signal block, and amplified by cryogenically cooled low-noise transistor amplifiers (LNTAs). Importantly, all devices inside the cryostat, including the feed, are cooled to 20 K, thus greatly reducing the inherent noise of the radio-telescope–radiometer system [8].

After being amplified by the LNTAs, the right-hand and left-hand circular polarized signals of the three frequency ranges are fed into the transformation channels, each of which operates in its own frequency range and with its own polarization. Channel functions include amplification, frequency transformation into the 1–2 GHz range, the formation of an output band at an intermediate frequency, and signal filtration. The receiving channels are synchronized from the radio-telescope frequency timing system.

Table 3. Technical characteristics of the telescopes.

Parameter	Current status	VLBI-2010
Operation time	24 hr, once a week	24 hrs a day
Restoration time	Up to several months	< 24 hr
Antenna diameter	5 – 100 m	$\approx 10-12$ m
Rotation rate	$\approx 20-200$ grad min^{-1}	$\geqslant 360$ grad min^{-1}
Frequency range	S/X	$\sim 2-15(18)$ GHz
Recording rate	128; 256 Mbit s^{-1}	8 – 16 Gbit s^{-1}
Data transfer	Disc transfer, e-VLBI * in some cases	e-VLBI, disc transfer in some cases
Number of stations	40 randomly distributed stations	40 optimally distributed stations
Number of stations equipped with: three measuring instruments four measuring instruments	 16 5	 40 20
* e-VLBI — so-called electronic, real-time VLBI.		

Figure 1. Antenna system of the RT-13 radio telescope.

Figure 2 shows a prototype of the in-cryostat wide-aperture triband feed, and Table 5 lists the parameters of the radio-telescope receiving antenna.

4. Frequency timing system

The frequency timing system (FTS) integrates frequency–time and coordinate–time measurements within the VLBI network, synchronizes telescopes with the start of information registration at the observation sites, and controls the phase characteristics of the receiving/recording system [9].

To transmit the reference frequency signal from the hydrogen standard to the radiotelescope, a fiber-optic line is used, with a feedback feature to ensure phase stability. Assuming a one-hour averaging period, the total instability introduced does not exceed 5×10^{-15}. The radio-telescope time scale PPS (pulse per second) signals and time code IRIG-B pulses (Inter-Range Instrumentation Group–Time Code Format B) are formed from a reference frequency signal using the second-long pulses of the GNSS receiver. We note that the observations of the VLBI observatories and the time registration of radio source observations are UTC-synchronized to within less than a microsecond.

The phase stability of the receiving/recording system is controlled by a phase calibration signal consisting of picosecond pulses. The picosecond pulse generator produces a phase calibration signal that is phase-locked to the reference frequency signal and consists of pulses with a repetition rate of 1 MHz and a duration of less than 20 ps, ensuring a spectrally continuous phase calibration signal at frequencies

Table 4. Key technical characteristics of the antenna system.

Radio telescope system	Mirror type, with secondary mirror
Receiver locations	Secondary focus, in a container
Antenna diameter	12 – 13 m
Frequency range (no less than)	2.0 – 40.0 GHz
Surface accuracy including secondary mirror (no worse than)	0.2 mm
Antenna temperature excluding the atmosphere (no more than)	10 K
Telescope surface efficiency factor in the 3–18 GHz frequency range (no less than)	0.7
Azimuth range	±270°
Elevation range	−5° – 90°
Azimuth rotation velocity (no less than) Acceleration (no less than)	12 grad s^{-1} 3 grad s^{-2}
Elevation rotation velocity (no less than) Acceleration (no less than)	6 deg s^{-1} 3 deg s^{-2}
Tracking precision (no worse than)	16 angular seconds
Ambient air temperature	from −40 °C to +50 °C
External influences	Rain, snow, hoarfrost, dew
Maximum working wind speed Maximum wind speed allowance	20 m s^{-1} 55 m s^{-1}
Number of rearrangements (no less than)	1000
Service life (including maintenance and repair)	20 years
Seismic influences	Horizontal acceleration 0.3*g*, Vertical acceleration 0.1*g*

Figure 2. Triband feed in a cryostat (without a radio transparent window).

up to about 40 GHz. Each spectral component of the calibration signal, together with the received signal, passes through the whole receiving/recording unit and is registered along with the valid signal.

5. Broadband digital data acquisition system

An important equipment element of "Quasar" telescopes is an analog signal transformation system [10]. To compensate for the telescope sensitivity loss due to the much smaller effective area of the antenna, the new Broadband Russian Acquisition System (BRAS) [11], is being developed based on the digital processing of the intermediate frequency (IF) signals from the inputs of radio astronomical receivers and using the module principle. The system consists of (i) eight identical modules of digital transformation channels (DTCs); (ii) a synchronization module; and (iii) an electrical power unit. The modules are connected by a cross plate, where the synchronization signals branch off from those controlling the DTC modules. The fact that the system has a common synchronization module ensures the synchronous formation of digital flows at the outputs of all eight BRAS channels. In each DTC, the 1.0–1.5-GHz input signals from the output of the corresponding receiving device are transformed into a digital information flow in the VLBI Data Interchange Format (VDIF), which is then transmitted via optical interface 10-G Ethernet to the radio telescope data buffer. The DTC components include an input filter to limit the bandwidth of the signal, an attenuator to set the channel input level, a high-speed ADC081500-type analog–digital converter (ADC), and a XC6SLX100T Spartan 6 programmable logic integrated microcircuit (PLIC). The PLIC measures the mean-square value of the signal, performs 2-bit digital quantization, forms a VDIF digital flow, and contains an output optical transceiver.

The synchronization module generates signals at clock frequencies of 1024 MHz (for ADC) and 256 MHz (for PLIC) and phase-locks them to the signals arriving from the FTS: reference frequency (100 MHz) signals and 1 Hz time-scale signals. Also, the synchronization module issues timestamps for VDIF digital flows and measures delays between the timestamps and the second-length pulses of the radio-telescope time scale (1 Hz of the time scale) and between the timestamps and the pulses from the receivers of the global navigation system (1 Hz GNSS).

The BRAS distributed control system is implemented with the DTC PLIC controllers and in the synchronization module. Intermodule control signals are transmitted via the UART (Universal Asynchronous Receiver/Transmitter) interface. The communication interface (Ethernet) with the radio-telescope control main computer is placed in the synchronization module. The transmission band of the BRAS channels has a maximum value of 512 MHz, which corresponds to a total velocity of 16 Gbps of the output 2 bit information flow (Table 6).

With module implementation using removable Europack standard modules, the system is easy to operate, and the vibration-resistant, electromagnetically screened $440 \times 310 \times 235$ mm housing enables placing BRAS in the telescope elevation unit. The AC–DC (alternating current–direct current) electric power unit from Delta Elektronika is placed in the same housing, together with the modules.

Experimental studies of the 2-channel BRAS prototypes (Fig. 3) confirmed the feasibility of the engineering and software solutions on which the project is based. Experimental implementations of BRAS will be deployed on RT-13 radio telescopes at the Zelenchukskaya and Badary "Quasar" observatories.

6. Buffering and data transfer for small antenna radio interferometers

For data to be transmitted in a real-time regime from observatories to the correlator, network and service equipment supporting the Ethernet standard will be deployed at observatories and at entries to the main communication channels.

A prototypical data buffering/transfer system (DBTS) has been developed based on two Dell R720 servers with two external Dell PV MD1220 arrays that ensure the connection of 24 accumulators (HDD), 2.5″ (SAS/SSD), in each of the arrays (Fig. 4). The connecting interfaces between the arrays and the server are SAS (Serial Attached SCSI (Small Computer System Interface)). Mounted on the servers is the UNIX operating system (Linux, Ubuntu version 12.04, with

Table 5. Receiving antenna parameters of the RT-13 radio telescope.

Range	Operating frequency range, GHz	Polarization	Noise temperature estimate	Directional diagram width of feed (−16 dB)	Number of BW subchannels	Operating regimes
S	2.2 – 2.6	Left and right circular	23.2	130°	2	1S + 3X 1X + 3Ka
X	7.0 – 9.5		29.7		6	
Ka	28 – 34		44.5		6	

Table 6. Basic BRAS parameters.

BRAS parameter	Value
Number of channels in the system	8
Channel pass band	512 MHz
Clock frequency for recording sampled digital signals	1024 MHz
Quantization type	2-bit
Net information flow speed at each channel output	2048 Mbps
Net information flow speed at each system output	16 Gbps
Data format at the system output	VDIF
Output interface	10 GE
Synchronization signals	100 MHz and 1 Hz
Control interface	Ethernet

the ext4 file system and FreeBSD-9.1 with ZFS (Zertabyte File System)).

Using this prototype, an hour-long record of the VLBI observation (60 radio source scans) of an actual 16 Gbps data flow has been modeled. Further, an estimate was made of the data transfer speed between fiber-optically connected servers with a 10 Gbps data throughput via a c4900M commutator using the high-speed Tsunami-UDP protocol.

The recording speed of the 60-scan one-hour model (data emulation from eight 10 GB channels of a broadband signal conversion system, a total of 80 GB) was about 20 Gbps.

7. Software correlator for processing data from the next-generation radio interferometer

From the standpoint of preliminary processing systems, it is mainly the broader band frequency channels and the fact that the data enter the correlator faster that make the next-generation interferometer special. At each station, quasar signals are 2-bit digitized and registered in four-frequency channels as either single or double polarized, with the respective transmission bandwidths of 1024 MHz and 512 MHz.

A major effort is underway to develop a next-generation correlator capable of processing small antenna VLBI data [12] from six stations at once in a quasi-real-time manner. The data processing rate and the data input rate to the correlator have the same average value up to 97 Gbp s^{-1}. To filter out narrow-band noise in frequency channels with broad pass bands, a task is given to the correlator to calculate the cross-spectra of VLBI signals with the high resolution up to 4096 spectral points.

To process VLBI data, an algorithm called FX (Foreign Exchange) is chosen, which improves the resolution of the calculated cross-spectra without greatly increasing the computational effort. The correlator is being developed as a software one, i.e., only standard mass-produced computational systems are used as its software components. The key distinguishing feature of the VLBI correlator being developed, in contrast to its existing counterparts, is that it uses Nvidia Tesla graphic processor accelerators (GPAs) to

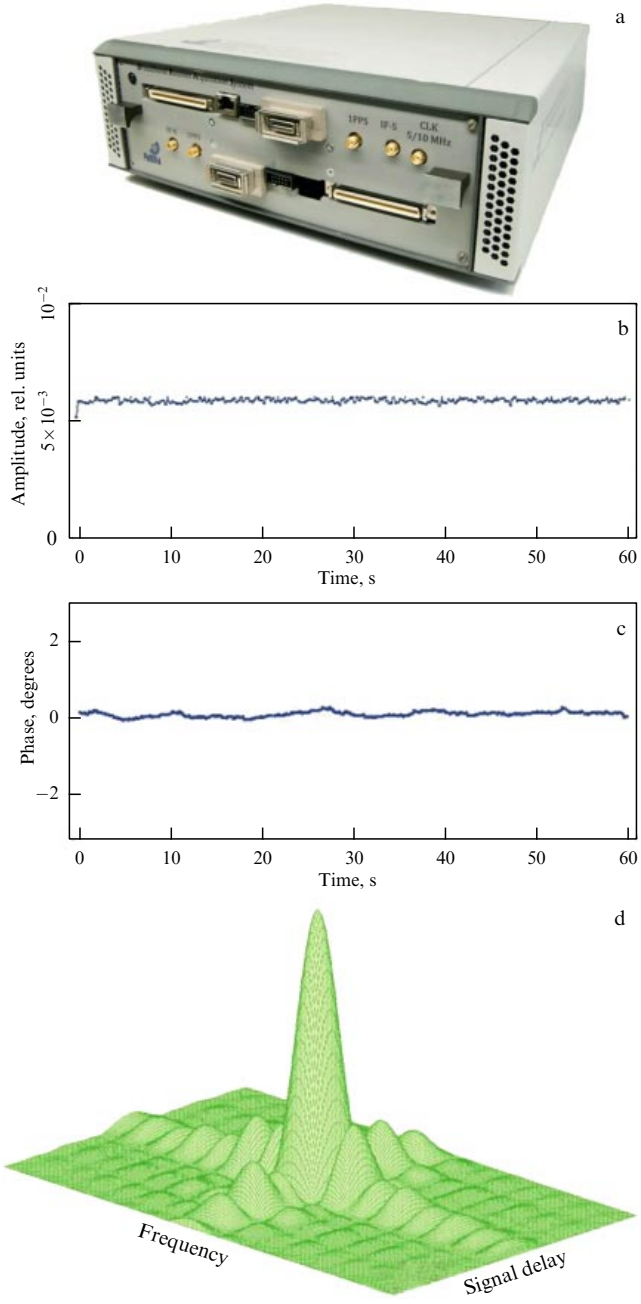

Figure 3. (a) Prototype showing channels of a broadband digital signal conversion system. Correlation response: (b) amplitude, (c) phase, and (d) example shape of a power spectrum module, from the 21 September 2012 Svetloye–Zelenchukskaya observation of the 0059 + 581 source in the 512 MHz band in the X frequency range using the developed models.

implement the most laborious computations: the separation of the PPG (picosecond pulse generator) signals and the determination of the cross-correlation spectra. With GPAs, a considerable reduction in size can be achieved for the correlator software.

The hardware chosen was a processor cluster on V200F hybride blade servers made by T-Platformy Corp., each containing two Intel® Xeon® E52600 CPUs and two NVIDIATesla® class M GPAs. The local, high-speed InfiniBand standard network interconnecting the blade servers via a Mellanoc switch enables a data exchange with the rate up to 56 Gbps between any pair of blades.

Figure 4. (a) Prototype of a data buffering and transfer system. (b) Double-channel broadband signal converter.

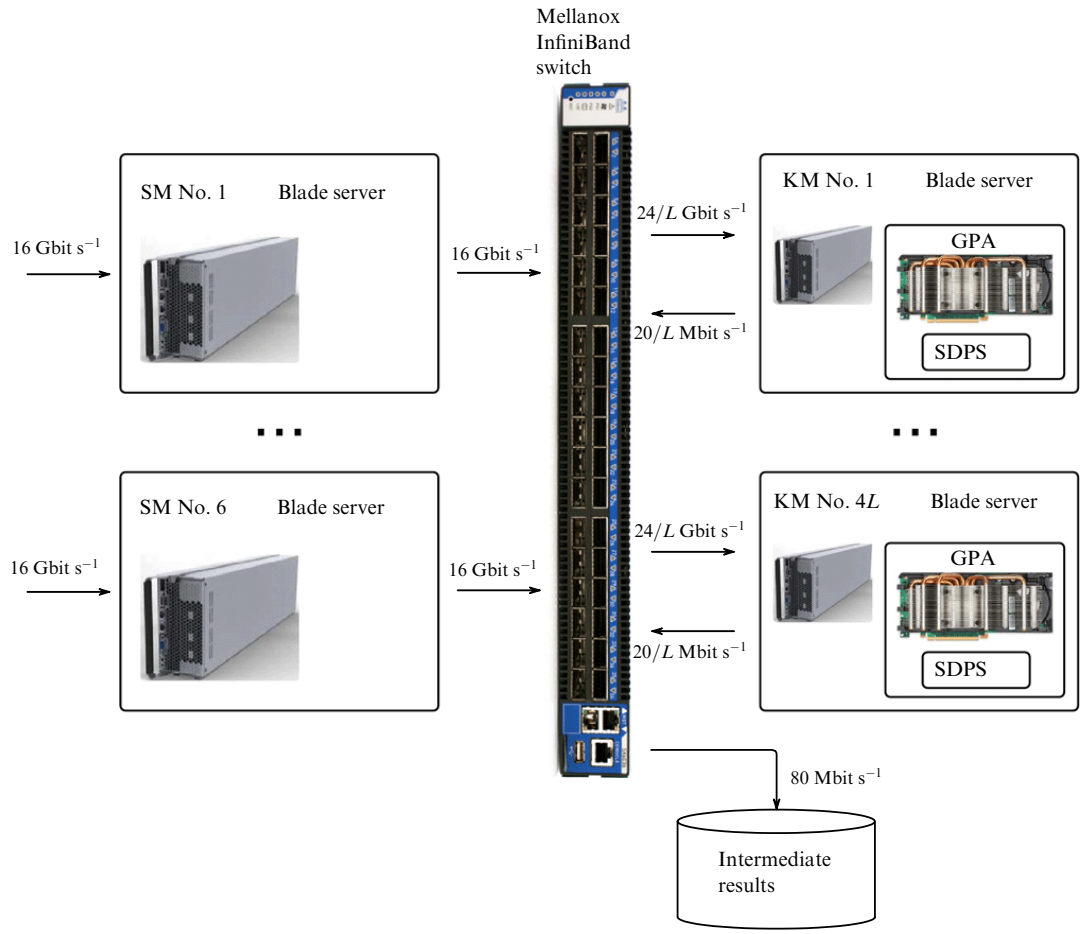

Figure 5. Hardware and software support of a six station correlator: structure and interaction.

The correlator software includes that for specifying the processing assignment, that for processing high-speed input data flows, and postprocessor software. The second (and the most complex of these) is illustrated in Fig. 5 in terms of its structure and interaction with the correlator hardware. There are several types of modules involved in the software. Computational modules are station and correlation types (SN and CM), either type using a single blade server. The number of station modules equals the number of stations, the data from each station being processed by a single module. The signals are decoded and shifted by the geometric delay of the station. The shifting procedure is carried out by the blade-server random access memory (RAM) unit, whose capacity of 64 Gbytes allows the data collection time 30 s. If required, the accumulated data can be stored in the cluster read-only memory (ROM) unit. The station module output flow transmitted over InfiniBand is equal to the 16 Gbps input flow.

The data are then fed to the correlation modules, each of which receives the same-range data from all the stations, resulting in 24 Gbps for the total flow of such data summed all of the modules. Each frequency range is processed by a total of $L < 10$ modules. A correlation module receives a block of data for the period of accumulation, for example, 1 s. The

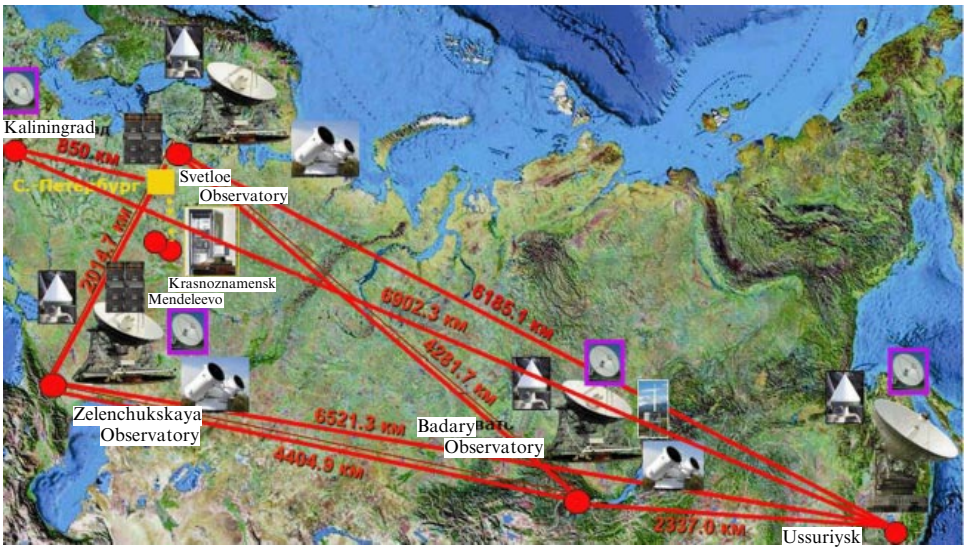

Figure 6. The VLBI "Quasar" system, 2020.

next block receives data from the next accumulation period, etc. By the time the data arrive at the Lth module, the first module has processed its data block, unloaded the results, and prepared to receive the next block.

In the correlation module, the data are processed in the GPA by specially designed spectral data processing software (SDPS), providing the cross-correlation functions and separating GPA signals. The results obtained with PPG — data flows up to 20 Mbps per frequency range on average — are downloaded to the RAM of the correlation modules, transmitted to the Raid array of the processor cluster, and then stored. Finally, the exactly calculated values of the group delays are transmitted to the data processing and analysis center.

8. Measurement system for atmospheric electrical characteristics

The measurement system for atmospheric electrical characteristics (MSAEC) is a hardware–software system intended for nearly real-time measuring of the varying component of the tropospheric signal propagation delay due to variations in the integral content of water vapor along the line of sight of the antenna [13]. The definition of the tropospheric delay is based on the fact that the varying component of the tropospheric delay is a function of the integral moisture content on the line of sight of the antenna, as is the troposphere brightness temperature at wavelengths close to the resonance frequency of water vapor (22.235 GHz).

Implemented standardly for this class of devices, MSAEC features a 500 MHz bandwidth radiometer with operating frequencies 20.4 GHz and 31.7 GHz with a built-in power calibration tool for received signals, plus two horn-lens antennas whose directivity can be varied within 180° using a plane rotating periscope mirror mounted at 45° to the horizon. The directivity diagram half-width of the antenna feed horns is 6°. The azimuthal turntable mounting of MSAEC enables the horn-lens antenna to be oriented to any point in the half-space.

Both radiometer channels share the same design scheme featuring two ferrite Y-switches at the input of the high-frequency block; from the switches, the antenna signals are sent to the low-noise amplifier input, as is, intermittently, one of the two matched calibration loads, a 'cold' one, which is at the temperature $T_1 = 40.000 \pm 0.007\,^{\circ}\mathrm{C}$, and a 'warm' one, at $T_2 = 65.000 \pm 0.007\,^{\circ}\mathrm{C}$. As a low-noise amplifier, volume-produced converters of signals into a range of intermediate frequencies are used. Mounted on the converter inputs are a sub-block containing intermediate-frequency amplifiers, quadratic detectors, and detector current amplifiers (whose inputs are fed into the data acquisition system).

We note that the error in measuring the relative delay variation is at most 0.5 K (with an effective signal averaging time of 1 s), a major portion of this being due to the sensitivity to changes in the atmosphere brightness temperature and due to the instability of the radiometer parameters.

9. Conclusion

When modernized under the project reviewed, the VLBI network "Quasar" system (Fig. 6) will be able to carry out fundamental submillimeter research and to perform sub-10-μs precision real-time determinations of the universal time required for the GLONASS. In another spin-off benefit, general modernization will allow the "Quasar" system to operate within next-generation global international networks for monitoring EOPs and reference frames.

References

1. Finkelshtein A M et al., in *Trudy Instituta Prikladnoi Astronomii RAN* (Proc. of the Institute of Applied Astronomy, Russian Academy of Sciences) Iss. 13 (Ed. A M Finkel'shtein) (St. Petersburg: Nauka, 2005) p. 7
2. Federal'naya Tselevaya Programma "Podderzhanie, Razvitie i Ispol'zovanie Sistemy GLONASS na 2012 – 2013 Gody", Utverzhdena Postanovleniem Pravitel'stva Rossiiskoi Federatsii No. 189 ot 3 Marta 2012 g. (Federal Program "Support, development and operation of the GLONASS for 2012 – 2020", Russian Federation Government Resolution No. 189 of 3 March 2012)
3. Finkelshtein A M et al., in *Trudy Instituta Prikladnoi Astronomii RAN* (Proc. of the Institute of Applied Astronomy, Russian Academy of Sciences) Iss. 23 (Ed. A V Ipatov) (St. Petersburg: Nauka, 2012) p. 55
4. Dick W R, Richter B (Eds) *IERS Annual Report 2008-09* (Intern. Earth Rotation and Reference Systems Service, Central Bureau)

(Frankfurt am Main: Verlag des Bundesamts für Kartographie und Geodäsie, 2012), Electronic version published on December 23, 2011
5. Plag H-P, Pearlman M (Eds) *Global Geodetic Observing System: Meeting the Requirements of Global Society on a Changing Planet in 2020* (New York: Springer, 2009)
6. Hase H et al., in *Measuring the Future. Proc. of the Fifth IVS General Meeting* (Eds A Finkelstein, D Behrend) (St. Petersburg: Nauka, 2008) p. 109
7. Ipatov A V, Chernov V K, in *Trudy Instituta Prikladnoi Astronomii RAN* (Proc. of the Institute of Applied Astronomy, Russian Academy of Sciences) Iss. 21 (Ed. A M Finkelshtein) (St. Petersburg: Nauka, 2010) p. 69
8. Ipatov A V, in *Trudy Instituta Prikladnoi Astronomii RAN* (Proc. of the Institute of Applied Astronomy, Russian Academy of Sciences) Iss. 2 (Ed. A M Finkelshtein) (St. Petersburg: Nauka, 1997) p. 232
9. Karpichev A S, Ivanov D V, in *Trudy Instituta Prikladnoi Astronomii RAN* (Proc. of the Institute of Applied Astronomy, Russian Academy of Sciences) Iss. 24 (Ed. A V Ipatov) (St. Petersburg: Nauka, 2012) p. 233
10. Ipatov A V, Kol'tsov N E, Fedotov L V *Prib. Tekh. Eksp.* (6) 140 (2006)
11. Fedotov L V, in *Trudy Instituta Prikladnoi Astronomii RAN* (Proc. of the Institute of Applied Astronomy, Russian Academy of Sciences) Iss. 24 (Ed. A V Ipatov) (St. Petersburg: Nauka, 2012) p. 165
12. Surkis I F et al., in *Trudy Instituta Prikladnoi Astronomii RAN* (Proc. of the Institute of Applied Astronomy, Russian Academy of Sciences) Iss. 24 (Ed. A V Ipatov) (St. Petersburg: Nauka, 2012) p. 172
13. Bykov V Yu, Il'in G N, Kaidanovskii M N, in *Trudy Instituta Prikladnoi Astronomii RAN* (Proc. of the Institute of Applied Astronomy, Russian Academy of Sciences) Iss. 21 (St. Petersburg: Nauka, 2010) p. 255